

# Structure and Chemical Sensing Applications of Zirconium Acetate Sol-Gel Films

Gregory O. Noonan and Jeffrey S. Ledford\*

Department of Chemistry, The Center for Fundamental Materials Research,  
Michigan State University, East Lansing, Michigan 48824-1322

Received October 18, 1994. Revised Manuscript Received April 13, 1995<sup>⊙</sup>

Zirconium acetate polymer oxide glass thin films have been prepared by hydrolysis of zirconium(IV) *n*-propoxide in excess acetic acid. Fourier transform infrared spectroscopy and X-ray photoelectron spectroscopy (XPS) have been used to determine the structure of the films. Results of spectroscopic analysis show that the polymer film consists of a Zr-O backbone coordinated with bridging and chelating bidentate acetate ligands. XPS data indicate that approximately 1.1 acetate ligands/Zr center are present in the film. The alcohol and alkane sorption properties of the film have been determined using a quartz crystal microbalance. Our results show that the zirconium acetate film sorbs alcohols and rejects alkanes. The alcohol affinity of the film has been attributed to hydrogen bonding interactions between the alcohol hydroxyl group and O atoms (Zr-O backbone and acetate ligands) in the zirconium acetate polymer. For alcohols larger than ethanol, repulsive interactions between the alkyl portion of the molecule and the polar film appear to limit alcohol sorption.

## Introduction

The development of new materials that can improve the analytical capabilities of sensor devices is an important part of chemical sensor research. One promising method for constructing such materials involves the combination of selective molecular recognition centers with functional host matrices. While considerable attention has been given to the study of sophisticated recognition centers,<sup>1-6</sup> relatively little effort has been devoted to the development of host matrices that complement or even improve the performance of the sensor. Greater control over matrix properties would be advantageous in many sensor applications. For example, control of chemical affinity and/or matrix pore structure would allow concentration of desired analytes and rejection of species that would interfere with or poison the active site of the sensor.

The sol-gel process is an attractive approach for the preparation of sensing materials because porous, optically transparent thin films of high purity can be synthesized at low temperatures. These polymer oxide glasses have been used to construct chemical sensors based on optical,<sup>7-13</sup> mass,<sup>14-18</sup> and conductimetric<sup>19,20</sup>

transduction methods. In these studies the gel has been used primarily as an immobilization matrix for selective interaction sites such as porphyrins,<sup>9,12</sup> cyclodextrins,<sup>13</sup> cryptates,<sup>10</sup> and organometallic compounds.<sup>8</sup> In addition, Bein et al.<sup>14,17,18</sup> have reported that zeolite/glass composite films exhibit molecular exclusion properties. However, the molecular sieving properties of these composites were attributed primarily to the zeolite component of the films. Only limited effort has been devoted to using sol-gel chemistry to prepare host matrices which can enhance the selectivity, sensitivity, or stability of the composite sensor material.

Metal carboxylate polymer matrices prepared using sol-gel methods have shown promise in a variety of sensor applications,<sup>8-12</sup> but the chemical and physical properties of the materials have not been extensively investigated. This work is part of a larger study devoted

\* Abstract published in *Advance ACS Abstracts*, May 15, 1995.

(1) Vogtle, F. *Introduction to Supramolecular Chemistry*; John Wiley & Sons, Inc.: New York, 1991.

(2) Seel, C.; Vogtle, F. *Angew. Chem., Int. Ed. Engl.* **1992**, *31*, 528.

(3) An, H.; Bradshaw, J. S.; Izatt, R. M. *Chem. Rev.* **1992**, *92*, 543.

(4) Gokel, G. *Crown Ethers and Cryptands*; Stoddart, J. F., Ed. In *Series in Monographs in Supramolecular Chemistry*; Royal Society of Chemistry: Cambridge, England, 1989.

(5) Gutsche, C. D. *Calixarenes*; Stoddart, J. F., Ed. In *Series in Monographs in Supramolecular Chemistry*; Royal Society of Chemistry: Cambridge, England, 1989.

(6) Lehn, J. M. *Angew. Chem., Int. Ed. Engl.* **1988**, *27*, 89.

(7) Avnir, D.; Levy, D.; Reisfeld, R. *J. Chem. Phys.* **1984**, *88*, 5956.

(8) Dulebohn, J.; Haefner, S.; Berglund, K. A.; Dunbar, K. *Chem. Mater.* **1992**, *4*, 506.

(9) Lessard, R. B.; Wallace, M. M.; Oertling, W. A.; Chang, C. K.; Berglund, K. A.; Nocera, D. G. In *Processing Science of Advanced Ceramics*; Aksay, A. I., McVay, G. L., Ulrich, D. R., Eds.; Mater. Res. Symp. Proc. 155; MRS: Pittsburgh, PA, 1989; p 109.

(10) Dulebohn, J. I.; VanVlierberge, B.; Berglund, K. A.; Lessard, R. B.; Yu, J.; Nocera, D. G. In *Better Ceramics Through Chemistry IV*; Zelinsky, B. J. J., Brinker, C. J., Clark, D. E., Ulrich, D. R., Eds.; Mater. Res. Soc. Proc. 180; MRS: Pittsburgh, PA, 1990; p 733.

(11) Newsham, M. D.; Cerreta, M. K.; Berglund, K. A.; Nocera, D. G. In *Better Ceramics Through Chemistry III*; Brinker, C. J., Clark, D. E., Ulrich, D. R., Eds.; Mater. Res. Soc. Proc. 121; MRS: Pittsburgh, PA, 1988; p 627.

(12) Dunuwila, D. D.; Torgerson, B. A.; Chang, C. K.; Berglund, K. A. *Anal. Chem.* **1994**, *66*, 2739.

(13) Berglund, K. A.; Nocera, D. G., unpublished work.

(14) Yan, Y.; Bein, T. *J. Chem. Phys.* **1992**, *96*, 9387.

(15) Frye, G. C.; Martin, S. J.; Ricco, A. J.; Brinker, C. J. In *Better Chemical Sensors and Microinstrumentation*; ACS Symp. Ser. 403; ACS: Washington, DC, 1989; p 208.

(16) Frye, G. C.; Martin, S. J.; Ricco, A. J.; Brinker, C. J. In *Better Ceramics Through Chemistry III*; Brinker, C. J.; Clark, D. E.; Ulrich, D. R., Eds.; Mater. Res. Soc. Proc. 121; MRS: Pittsburgh, PA, 1988; p 349.

(17) Bein, T.; Brown, K.; Frye, G. C.; Brinker, C. J. *J. Am. Chem. Soc.* **1989**, *111*, 7640.

(18) Bein, T.; Brown, K.; Enzel, P.; Brinker, C. J. In *Better Ceramics Through Chemistry III*; Brinker, C. J., Clark, D. E., Ulrich, D. R., Eds.; Mater. Res. Soc. Symp. Proc., 121; MRS: Pittsburgh, PA, 1988; p 761.

(19) Yoshimura, N.; Sato, S.; Itoi, M.; Taguchi, H. *Sozai Bussseigaku Zasshi* **1990**, *3*, 47.

(20) Inubushi, A.; Masuda, S.; Okubo, M.; Matsumoto, A.; Sadamura, H.; Suzuki, K. In *High Tech Ceramics*; Vincenzini, P., Eds.; Elsevier Science Publishers: Amsterdam, 1987; p 2165.

to designing transition-metal carboxylate polymer thin films for chemical sensor applications. We are interested in qualitatively and quantitatively defining the structure of these materials and subsequently correlating structural information with film properties that are important for chemical sensing. In this study, Fourier transform infrared spectroscopy (FTIR) and X-ray photoelectron spectroscopy (XPS) have been used to determine the structure of a zirconium acetate thin film prepared from zirconium(IV) *n*-propoxide and acetic acid. The information obtained from spectroscopic measurements has been compared to the acoustic sensor response of the film to alcohols and alkanes. The effect of film structure on sensor properties has been evaluated based upon these results.

### Experimental Section

**Materials.** Zirconium(IV) *n*-propoxide (70% in *n*-propanol), acetic acid, and *n*-propanol were obtained from Aldrich Chemical Co. and used without further purification. Analytes were chosen to study analyte/film interactions for *n*-alkanes and alcohols with different steric limitations. Analytes were obtained from either EM Science Co. or Aldrich Chemical Co. and used as received.

**Film Preparation.** The method used to synthesize the film was based on techniques used in these laboratories for the preparation of transition-metal carboxylate thin films.<sup>21</sup> Each solution and film were prepared in triplicate. Reactions were carried out at room temperature in capped vials. Molar ratios of acetic acid:water:alkoxide of 3:13.9:1 were used. The synthesis involved mixing 0.29 mL of acetic acid with 0.76 mL of zirconium *n*-propoxide in *n*-propanol, diluting the acetic acid/alkoxide solution with *n*-propanol (12 mL added to ~1 mL of solution), and finally adding 0.42 mL of water. A vortex mixer was used to vigorously stir solutions following the addition of each reactant. The reaction between acetic acid and zirconium *n*-propoxide was exothermic and the resulting zirconium solutions were clear and colorless. Films were deposited by spray coating fresh solutions onto the desired substrate (quartz or KBr). The films were air-dried overnight and stored in a desiccator. All films prepared in this study were transparent, colorless, and exhibited complete and uniform coverage of all substrates.

**Fourier Transform Infrared Spectroscopy (FTIR).** FTIR spectra of films spray coated onto KBr windows were obtained using a Mattson Instruments Galaxy 3020 Fourier transform infrared spectrometer. The mid-IR region (4000–400 cm<sup>-1</sup>) was examined with a resolution of 2 cm<sup>-1</sup>. Data acquisition and processing were performed using an Enhanced First software package.

**X-ray Photoelectron Spectroscopy (XPS).** Films cast on quartz slides (used as received) were analyzed with a Perkin-Elmer surface science instrument equipped with a Model 10-360 precision energy analyzer and an omnifocus small spot lens. All spectra were collected using a Mg anode (1253.6 eV) operated at a power of 300 W (15 kV and 20 mA) with an analyzer pass energy of 50 eV. The C 1s, O 1s, and Zr 3d regions were scanned for each film. Binding energies were referenced to ligand alkyl and adventitious carbon (C 1s = 284.6 eV). Empirically derived sensitivity factors<sup>22</sup> were used for quantitative XPS calculations involving the C 1s and O 1s. For the Zr 3d, sensitivity factors were derived from the analysis of ZrO<sub>2</sub> (Aldrich Chemical Co., 99.99+%). XPS peaks were fitted with 20% Lorentzian–Gaussian mix Voigt functions using a nonlinear least-squares curve-fitting program.<sup>23</sup> Each reported result is based on the analysis of at least three

films. It must be noted that the use of XPS to evaluate film composition assumes that the films are homogeneous.

**Sensor Test Apparatus.** Pulse measurements are performed using a heated gas chromatograph injector and heated transfer line to introduce analytes to the sensor test cell. The injector is operated at 250 °C to ensure complete vaporization of all the compounds. The transfer line is constructed from 3.5 in. long, 1/16 in. i.d. stainless steel tubing. It is held at 150 °C using a nichrome wire heater. The quartz crystal microbalance is housed in a small volume test cell (8 mL). Typical operating conditions are 20 cm<sup>3</sup>/min flow of dry nitrogen (99.95%, AGA Gas Co.) and test cell temperature of 30 °C. The temperature of the test cell was controlled by heat flow from the injector and transfer line. The injection volume used for the set of analytes varied from 0.1 to 3.0 μL in order to maintain frequency shifts of less than 150 Hz. At least three injections of each analyte were made to ensure reproducibility. Analyte injection order was varied to minimize the effect of analyte order on sensor response. The peak shape for each analyte consists of a sharp leading edge that appears 15 s after analyte injection, a narrow peak maximum (approximately 2 s), and a tailing return to baseline. The time required for the frequency to return to baseline was less than 2 min for the alkanes and approximately 6 min for the alcohols.

Equilibrium measurements are performed using a vapor generation system and operating procedures that have been detailed elsewhere.<sup>24</sup> Analyte concentration is controlled by adjusting the relative flow rates of carrier gas through a bubbler containing the analyte and a dilution gas line. Vapor concentrations are measured using an in-line 5 mL sample loop connected to a Varian 3700 GC equipped with a flame ionization detector. Vapor concentrations were maintained at 10<sup>-4</sup>–10<sup>-5</sup> mol/L in order to produce frequency shifts of less than 150 Hz. Each run consists of a 2 min nitrogen purge, vapor exposure for a period of time necessary for the QCM response to equilibrate, and a nitrogen purge equal to the time necessary for vapor/film equilibration.

**Quartz Crystal Microbalance (QCM).** Bulk acoustic wave measurements were performed using 6 MHz quartz crystal microbalances from Maxtek Inc. (Torrance, CA). A Model TM-100 thickness monitor (Maxtek Inc.) was used to determine the mass of the polymer coating and the response of the sensor to probe analytes. The output voltage of the thickness monitor (3.06 mV = 1 Hz) was recorded on a Hewlett-Packard 3394A integrator. The sensitivity of the QCM is 140 Hz/μg. QCM operating principles and their application to chemical sensing have been discussed extensively elsewhere.<sup>25–27</sup>

Quartz oscillators were soaked in 2-propanol, rinsed with methanol, and dried in air prior to use. Cleaned devices were placed in the oscillator circuit and the thickness monitor set to zero. The oscillators were spray coated with the polymer solution and allowed to dry. Films of approximately 0.4 μm thickness (~61 μg) were used in this study.

### Results and Discussion

**Structure of Zirconium Acetate Film.** The variety of reactions that occur in the polymer solutions could result in the coordination of several different ligands (e.g., alkoxides, carboxylates, esters, hydroxides, alcohols, and water) to the metal centers in the cast films. We have found that the structural information available from FTIR and the qualitative and quantitative capabilities of XPS provide significant insight into the composition of metal carboxylate films.<sup>21,28</sup>

(24) Townsend IV, E. B. Ph.D. Thesis, Michigan State University, 1995.

(25) Lu, C.; Czanderna, A. W. *Applications of Piezoelectric Quartz Crystal Microbalances*; Elsevier: Amsterdam, 1984.

(26) Grate, J. W.; Martin, S. J.; White, R. M. *Anal. Chem.* **1993**, *65*, 940A–948A.

(27) Grate, J. W.; Martin, S. J.; White, R. M. *Anal. Chem.* **1993**, *65*, 987A–996A.

(21) Severin, K. G.; Ledford, J. S.; Torgerson, B. A.; Berglund, K. A. *Chem. Mater.* **1994**, *6*, 890.

(22) Wagner, C. D.; Davis, L. E.; Zeller, M. V.; Taylor, J. A.; Gale, L. H. *Surf. Interface Anal.* **1981**, *3*, 211.

(23) Software provided by Dr. Andrew Proctor, University of Pittsburgh, Pittsburgh, PA.

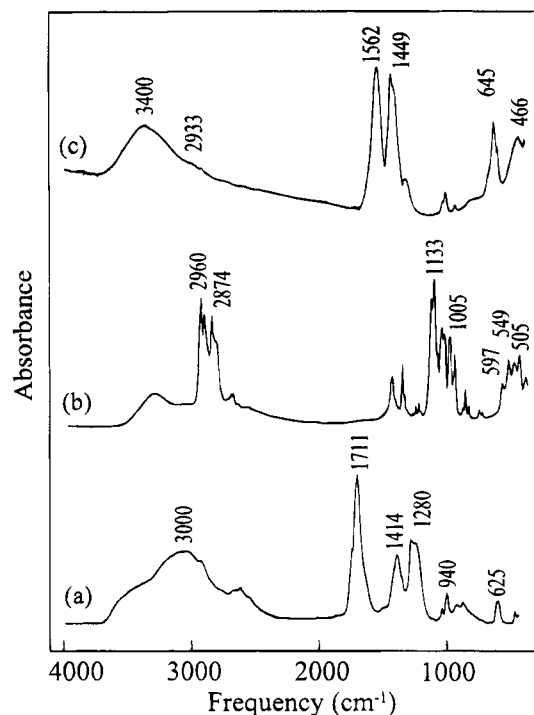


**Figure 1.** FTIR spectra of (a) acetic acid, (b) zirconium(IV) *n*-propoxide in *n*-propanol, and (c) zirconium acetate film.

**FTIR Spectra.** FTIR spectra of acetic acid, zirconium(IV) *n*-propoxide (in *n*-propanol), and the zirconium acetate film are shown in Figure 1. The assignment of spectral features for acetic acid (Figure 1a) is straightforward.<sup>29,30</sup> Weak methyl C-H stretching absorbances are observed near 2900  $\text{cm}^{-1}$  superimposed on an O-H absorbance centered at 3000  $\text{cm}^{-1}$ . The strong absorbance observed at 1711  $\text{cm}^{-1}$  is due to a dimeric carboxylic C=O asymmetric stretch. Asymmetric and symmetric  $\text{CH}_3$  deformation modes are observed at 1414 and 1280  $\text{cm}^{-1}$ , respectively. Bending and stretching vibrations of the C-O-H groups are observed between 1440 and 900  $\text{cm}^{-1}$ . Skeletal vibrations are evident at 1382 and 625  $\text{cm}^{-1}$ .

The FTIR spectrum obtained for zirconium(IV) *n*-propoxide in *n*-propanol is shown in Figure 1b. The major absorbances are the C-H stretching vibrations at 2960, 2934, and 2874  $\text{cm}^{-1}$  and a feature at 1133  $\text{cm}^{-1}$  which we attribute to a combination of (C-O)Zr and skeletal stretches. The peak observed at 1005  $\text{cm}^{-1}$  is due to (C-O)Zr stretching and features observed at 597, 549, and 505  $\text{cm}^{-1}$  are attributed to alkoxide (Zr-O)C stretches. These features are similar to those reported by Barraclough<sup>31</sup> for zirconium(IV) isopropoxide: a C-O absorbance at 1011  $\text{cm}^{-1}$  and features between 590 and 520  $\text{cm}^{-1}$  due to alkoxide Zr-O stretches.

Figure 1c shows the FTIR spectrum measured for the zirconium acetate film. Three weak features characteristic of methyl stretches of the acetate ligand are observed at 3017, 2933, and 2980  $\text{cm}^{-1}$ . Less intense

bands observed between 1400 and 700  $\text{cm}^{-1}$  are due to C-C stretching and C-H bending vibrations of the acetate ligand. A broad band due to hydroxyl groups is observed near 3400  $\text{cm}^{-1}$ . The low-frequency region of the spectrum shows two major features at 645 and 466  $\text{cm}^{-1}$  which we attribute to Zr-O stretches. Atik and Aegerter<sup>32</sup> have attributed bands at 666 and 363  $\text{cm}^{-1}$  to Zr-O stretches in a zirconium acetate film.

The predominance of carboxylate ligand features observed in the FTIR spectrum of the film (Figure 1c) suggests that most of the ligands are acetate groups. In addition, no features attributable to ester or alkoxide ligands are observed in the FTIR spectrum. It should be noted that previous work on zirconium acetate gels<sup>32</sup> showed that acetate and alkoxide ligands were bound to the polymer backbone. It is possible that the excess acid used in our preparation increases the reactivity of the alkoxide ligands during the hydrolysis and condensation steps of the reaction. The enhanced reactivity would lead to a decrease in the number of alkoxide ligands present in the cast films. Doeuff et al.<sup>33</sup> reported that gelatinous precipitates prepared from excess acetic acid and titanium butoxide (Ac/Ti = 10) contained no alkoxide ligands.

**Carboxylate Coordination.** Previous studies of metal carboxylate coordination have compared the splitting between asymmetric and symmetric COO stretches with the splitting observed in the ionic form of the ligand to ascertain carboxylate coordination modes.<sup>34</sup> Splittings much larger than that observed for the ionic species tend to indicate monodentate ligands while smaller separations are considered characteristic of bidentate ligands. It has also been suggested that splittings significantly smaller than the ionic value are indicative of bidentate chelating coordination while separations closer to ionic values are typical of bidentate bridging coordination.<sup>35</sup> This reasoning has been used to determine acetate ligand coordination in the evolution of titanium xerogels<sup>33</sup> and in titanium, zirconium, and hafnium acetate solutions before and after the addition of water.<sup>36</sup>

Figure 2 shows the carboxylate stretch region of the FTIR spectra measured for the zirconium acetate film and sodium acetate. The asymmetric and symmetric COO stretch frequencies for sodium acetate (1580 and 1418  $\text{cm}^{-1}$ ,  $\Delta\nu = 162 \text{ cm}^{-1}$ ) are similar in relative intensity and position to those reported by Spinner.<sup>37</sup> In the film spectrum, the symmetric COO stretch is as broad as the asymmetric stretch; however, only one well-resolved maximum is observed at 1449  $\text{cm}^{-1}$ . The separation between the asymmetric and symmetric COO stretches ( $\Delta\nu = 113 \text{ cm}^{-1}$ ) is reported with respect to this maximum which is on the high-energy side of the peak. The asymmetric-symmetric splitting observed for the acetate film suggests that a majority of the acetate ligands are bidentate. Since the asymmetric

(32) Atik, M.; Aegerter, M. A. *J. Non-Cryst. Solids* **1992**, *147*, 148, 813.

(33) Doeuff, S.; Henry, M.; Sanchez, C.; Livage, J. *J. Non-Cryst. Solids* **1987**, *89*, 206.

(34) Mehrotra, R. C.; Bohra, R. *Metal Carboxylates*; Academic Press: London, 1983.

(35) Deacon, G. B.; Phillips, R. J. *Coord. Chem. Rev.* **1980**, *33*, 227.

(36) Gagliardi, C. D.; Berglund, K. A. In *Processing Science of Advanced Ceramics*; Aksay, A. I., McVay, G. L., Ulrich, D. R., Eds.; Mater. Res. Symp. Proc. 155; MRS: Pittsburgh, PA, 1989; p 127.

(37) Spinner, E. *J. Chem. Soc.* **1964**, 4217.

(28) Severin, K. G.; Ledford, J. S. *Langmuir*, in press.

(29) Colthup, N. B.; Daly, L. H.; Wiberley, S. E. *Introduction to Infrared and Raman Spectroscopy*, 3rd ed.; Academic Press: San Diego, 1990.

(30) Silverstein, R. M.; Bassler, C. G.; Morrill, T. C. *Spectrometric Identification of Organic Compounds*, 3rd ed.; John Wiley & Sons, Inc.: New York, 1974.

(31) Barraclough, C. G.; Bradley, D. C.; Lewis, J.; Thomas, I. M. *J. Chem. Soc.* **1961**, 2601.

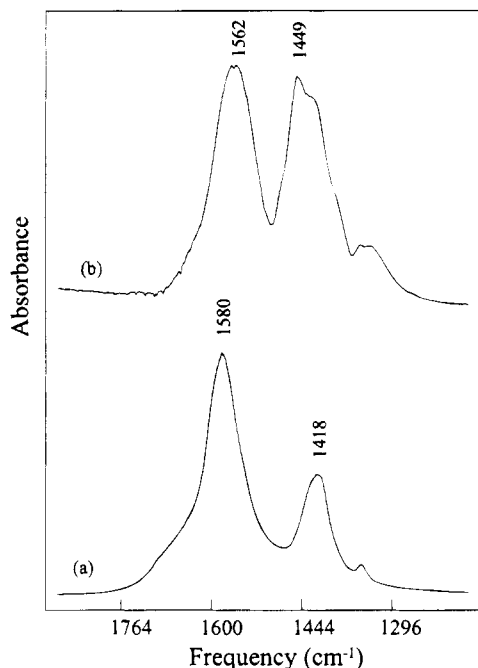


**Figure 2.** FTIR spectra of carboxylate region obtained for (a) sodium acetate and (b) zirconium acetate film.

and symmetric peaks are fairly broad, both bidentate bridging and chelating ligands are probably present. Atik and Aegerter<sup>32</sup> report values of 1578 and 1452  $\text{cm}^{-1}$  ( $\Delta\nu = 126 \text{ cm}^{-1}$ ) for the asymmetric and symmetric COO stretches of a zirconium acetate film, a separation also indicative of bidentate ligands.

**XPS Spectra.** The XPS Zr 3d<sub>5/2</sub> binding energy measured for the zirconium film (182.2 eV) is typical of values measured for tetravalent zirconium.<sup>38</sup> The XPS C 1s spectrum measured for the film consists of peaks at 284.6 eV (reference peak) and 288.9 eV due to alkyl and carboxylate carbon, respectively. No features due to alkoxide ( $\sim 286 \text{ eV}$ ) are observed in the spectra. The XPS O 1s spectrum measured for the film consists of peaks at 530.0 and 531.4 eV that may be attributed to backbone and ligand (acetate, hydroxyl, or water) oxygen, respectively. The carboxyl carbon/zirconium, backbone oxygen/zirconium, and ligand oxygen/zirconium atomic ratios calculated from C 1s, O 1s, and Zr 3d XPS peak intensities were 1.1, 1.5, and 2.5, respectively.

The atomic ratios derived from XPS intensity ratios provide a quantitative assessment of the number and type of ligands present in the film. The extent of carboxylate incorporation observed for the zirconium acetate film (1.1 acetates/zirconium) is similar to results obtained from TGA analyses of zirconium-based acetate gels.<sup>39</sup> Since each carboxylate carbon is associated with two ligand oxygens, a film containing only carboxylate ligands is expected to have a ligand oxygen/carboxyl carbon ratio close to 2. The ligand oxygen/zirconium atomic ratio calculated for the zirconium acetate film (2.5) suggests that there are approximately 0.3 oxygen ligand/zirconium center that cannot be attributed to acetate. FTIR and XPS analyses indicate that the only

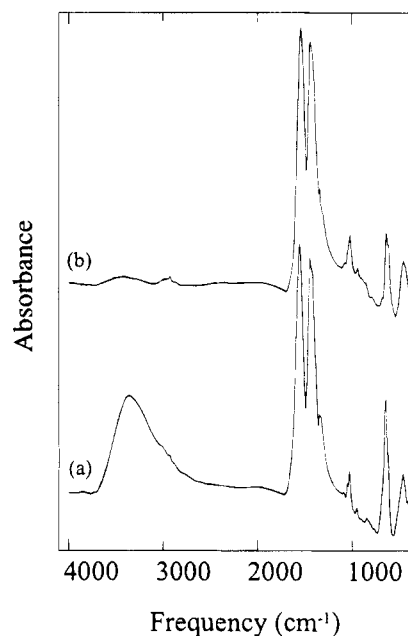


**Figure 3.** FTIR spectra of zirconium acetate film (a) before and (b) after heating to 100 °C.

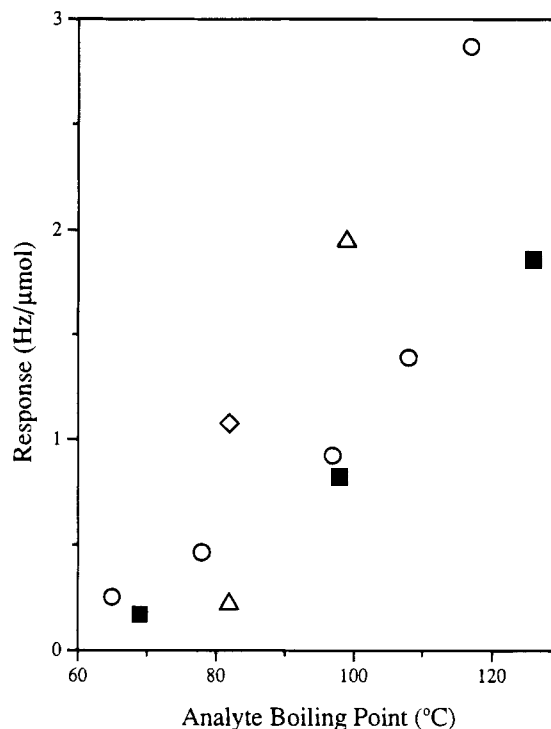


**Figure 4.** Variation of QCM pulse response ( $\text{Hz}/\mu\text{mol}$ ) versus analyte boiling point for uncoated quartz crystal. Analytes investigated are alkanes (■), primary alcohols (○), secondary alcohols (△), and *tert*-butyl alcohol (◇).

other possible oxygen-containing ligands present in the film are hydroxyl ligands or water. Water has a characteristic absorbance near 1640  $\text{cm}^{-1}$ .<sup>29</sup> Unfortunately, the strong carboxylate absorbances in this region make it impossible to use this feature to distinguish between hydroxyl ligands and water. Figure 3 shows the spectra of the zirconium acetate film before (a) and after (b) heating at low temperature (100 °C). It is obvious that the hydroxyl features are significantly diminished. Since it seems unlikely that hydroxyl ligands would be lost at such low temperatures, we attribute the excess ligand oxygen primarily to water

(38) *Handbook of X-ray Photoelectron Spectroscopy*; Wagner, C. D., Riggs, W. M., Davis, L. E., Moulder, J. F., Muilenburg, G. E., Eds.; Perkin-Elmer: Eden Prairie, MN, 1979.

(39) Leautic, A.; Riman, R. E. *J. Non-Cryst. Solids* **1991**, *135*, 259.

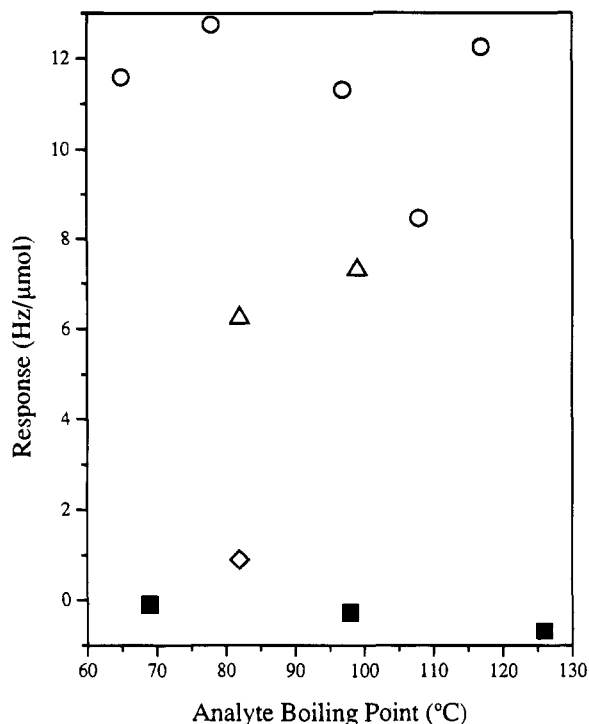


**Figure 5.** Variation of QCM pulse response (Hz/ $\mu\text{mol}$ ) versus analyte boiling point for zirconium acetate coated quartz crystal. Analytes investigated are alkanes (■), primary alcohols (○), secondary alcohols (△), and *tert*-butyl alcohol (◇).

sorbed in the film. This is consistent with previous work which indicated that zirconium acetate films were hydrophilic and water soluble.<sup>36</sup>

Using the XPS estimates of backbone oxygen and carboxylate ligand concentrations in the film, a general picture of the film structure can be proposed. Our results suggest that the zirconium acetate film consists of highly cross-linked networks of zirconium and oxygen, with most zirconium centers covalently bonded to three backbone oxygen atoms. In addition, if we assign a  $-2$  charge to backbone oxygen, a  $-1$  to the hydroxyl group, and a  $-1$  charge to the carboxylate group, the atomic ratios calculated from XPS lead to a total negative charge of  $-4.2$ . Within experimental error, this is the value expected for a neutral polymer involving a  $\text{Zr}^{4+}$  metal center. It must be noted that film stoichiometry determined by XPS cannot be used to determine the zirconium coordination number. It is likely that the acetate films have significant interchain interactions that lead to a coordination number greater than 5.

#### Sorption Properties of Zirconium Acetate Film.

Acoustic sensor responses are reported as the maximum frequency shift in hertz per micromole of analyte introduced ( $\text{Hz}/\mu\text{mol}$ ) to normalize the response for varying analyte concentrations. To emphasize the importance of physisorption, sensor responses are plotted versus analyte boiling point. A smooth exponential increase with increasing boiling point is expected for adsorption on a nonselective surface.<sup>40</sup> Deviations from this smooth trend are attributed to more selective analyte/film interactions.

Two types of response data are presented in this study. The zirconium acetate film response (Figure 5, Table 1) is defined as the difference between the

**Table 1. Analyte Pulse Responses on Acetate Coated and Uncoated QCM**

analyte	boiling point (°C)	symbol	response (Hz/ $\mu\text{mol}$ )		acetate/uncoated response ratio
			un-coated	acetate <sup>a</sup>	
methanol	65	○	0.49	12	46
hexane	69	■	0.33	-0.08	-0.47
ethanol	78	○	0.89	13	27
2-propanol	82	△	0.42	6.2	28
<i>tert</i> -butyl alcohol	82	◇	2.1	0.89	0.83
<i>n</i> -propanol	97	○	1.8	11	12
heptane	98	■	1.6	-0.26	-0.32
<i>sec</i> -butyl alcohol	99	△	3.8	7.3	3.8
2-butanol	108	○	2.7	8.5	76.1
<i>n</i> -butanol	117	○	5.5	12	4.2
octane	126	■	3.6	-0.68	-0.36

<sup>a</sup> Difference between coated and uncoated responses.

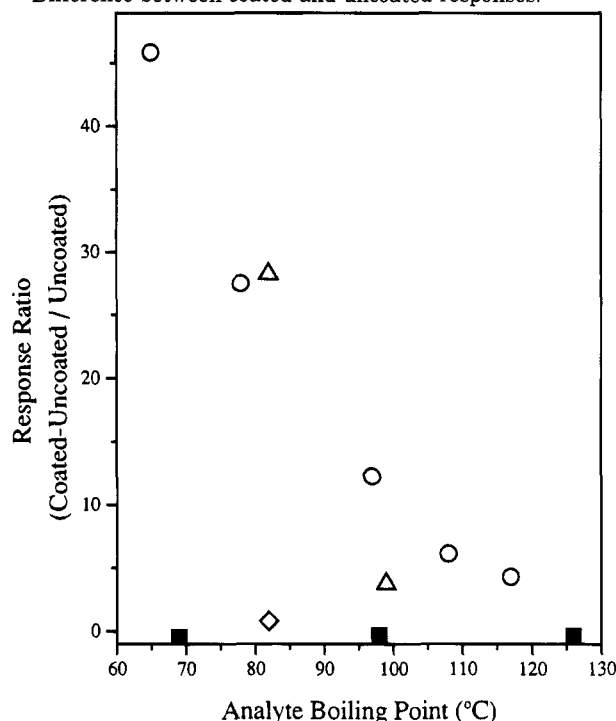


**Figure 6.** Variation of pulse response ratio (zirconium acetate coated crystal/uncoated crystal) versus analyte boiling point. Analytes investigated are alkanes (■), primary alcohols (○), secondary alcohols (△), and *tert*-butyl alcohol (◇).

responses measured for acetate-coated and uncoated QCM devices. Differences less than zero suggest a repulsive interaction between the coating and the analyte. A positive difference is indicative of analyte sorption into a coating. The response ratio for each analyte (Figure 6, Table 1) is defined as the difference response divided by the response measured with the uncoated crystal. Comparison of response ratios for different analytes can be used to assess the sorption selectivity of the coating.

**Pulse Response of Uncoated QCM Crystals.** Figure 4 and Table 1 show the variation in QCM response ( $\text{Hz}/\mu\text{mol}$ ) as a function of analyte boiling point for the uncoated quartz oscillator. The response of the uncoated device increases with increasing analyte boiling point. This indicates that the uncoated crystal does not selectively interact with either alkanes or alcohols and suggests that the response is strongly affected by analyte physisorption. King<sup>40</sup> proposed that a larger amount of partitioning would occur for higher boiling

(40) King, W. H., Jr. *Anal. Chem.* **1964**, *36*, 1735.

analytes exposed to coated quartz crystals. While partitioning cannot occur on the uncoated device, physisorption of the higher boiling analytes is expected to yield similar results.

**Pulse Response of Zirconium Acetate Coated QCM Crystals.** The variation in QCM response as a function of analyte boiling point for the zirconium acetate film coated device is shown in Figure 5 and Table 1. In contrast to the uncoated crystal results, the response for the zirconium acetate film does not depend only on analyte boiling point. The frequency shifts observed for the unbranched primary alcohols (open circles) are similar, within experimental error. It should be noted that for the uncoated crystal the response for *n*-butanol is over a factor of 10 greater than the methanol response. The response measured for 2-butanol (open circle, bp 108 °C), a branched primary alcohol, is lower than that observed for the other primary alcohols. For the secondary alcohols, 2-propanol and *sec*-butyl alcohol (open triangles), the measured responses are significantly lower than the values obtained for unbranched primary alcohols of comparable boiling point. The response for *tert*-butyl alcohol (open diamond) is lower than the responses measured for all the other alcohols. Alcohol responses are significantly higher than the values observed for alkanes (closed squares) with comparable boiling points. In addition, the alkane responses observed for the zirconium acetate film are approximately 30% lower than the values recorded for the uncoated crystal. Therefore, they exhibit negative values when corrected for the uncoated crystal response.

Comparison of the responses observed for primary alcohols and normal alkanes suggests that the acetate film interacts preferentially with alcohols. We attribute this enhanced alcohol response to hydrogen bonding interactions between the alcohol hydroxyl groups and the O atoms (Zr–O backbone and acetate ligands) in the film. The relatively small number of hydroxyl groups present in the film may also participate in hydrogen bonding interactions. The enhanced interaction between alcohols and the polymer serves as the driving force for migration of alcohols into the film. The negative alkane response may be attributed to repulsive interaction between the polar acetate film and the nonpolar hydrocarbons.

A more complete understanding of the sorption properties of the film may be obtained by examining the response ratio calculated for the zirconium acetate film. Figure 6 and Table 1 show the variation in the response ratio as a function of analyte boiling point. It should be noted that the alkane response ratios are negative and essentially independent of analyte. With the exception of *tert*-butyl alcohol and *sec*-butyl alcohol, the ratios calculated for the alcohols decrease dramatically from methanol to *n*-butanol. We attribute this trend to an increase in repulsive interactions between the nonpolar hydrocarbon portion of the alcohols and the polar acetate film. The deviation of the *tert*-butyl alcohol and *sec*-butyl alcohol response ratios from the general trend may be due to steric limitations expected for secondary and tertiary alcohols. The same deviation might also occur for 2-propanol; however, we believe that the low 2-propanol response measured with the uncoated QCM artificially increases the response ratio.

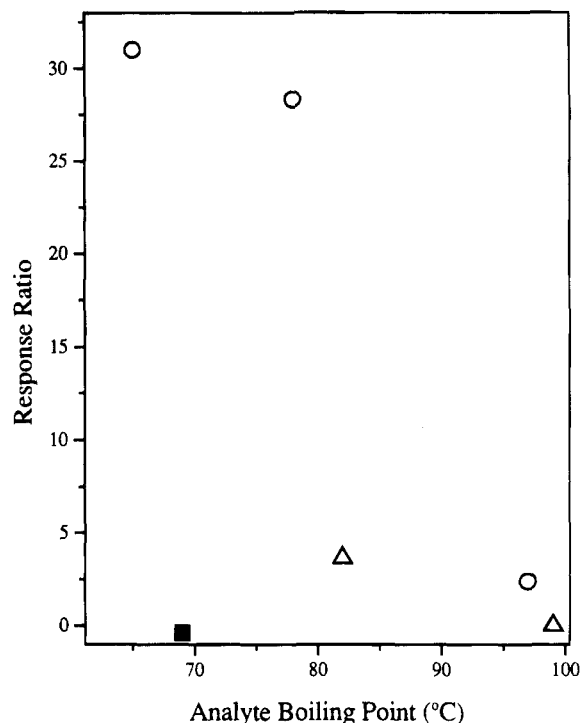


**Figure 7.** Variation of equilibrium response ratio (zirconium acetate coated crystal/uncoated crystal) versus analyte boiling point. Selected analytes are hexane (■), methanol, ethanol, *n*-propanol (○), and secondary alcohols (△).

**Equilibrium Response of Zirconium Acetate Coated QCM Crystals.** Pulsed sample introduction is an important technique for many sensor applications; however, it may convolute differences in analyte diffusion rates with analyte/film partition ratios. To determine the effect of analyte diffusivity on our evaluation of film properties, responses have been measured for films that have equilibrated with selected alcohol and alkane vapor streams. Figure 7 shows the variation in the equilibrium response ratio as a function of the boiling point of selected analytes. These ratios have been calculated using equilibrium responses measured for the uncoated QCM crystal. The equilibrium response ratios determined for methanol and ethanol are comparable and significantly higher than the values measured for the other analytes (*n*-propanol, 2-propanol, *sec*-butyl alcohol, and hexane). These results demonstrate that differences in analyte diffusivity affect the response trend determined using pulsed sample introduction.

Figure 8 shows the variation of normalized sensor response measured following exposure of the film to vapor streams of methanol, ethanol, and *n*-propanol. Similar studies with uncoated devices have shown that all the alcohols equilibrate with the QCM approximately 60 s after exposure to the alcohol stream. Figure 8 clearly shows that methanol equilibrates with the zirconium acetate film more rapidly than ethanol. Therefore, in a pulse injection system, this difference in equilibration times could result in a low response for ethanol compared to methanol.

Figure 8 also shows that *n*-propanol equilibrates with the film more rapidly than ethanol. Frye et al.<sup>41</sup> have reported that the diffusion coefficients of alcohols in

(41) Frye, G. C.; Martin, S. J.; Ricco, A. J. *Sens. Mater.* **1989**, *1-6*, 335.

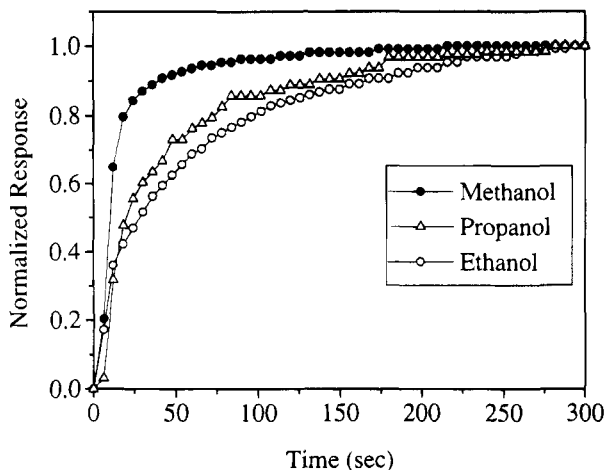


**Figure 8.** Normalized QCM response measured following exposure to vapor streams of methanol (●), ethanol (○), and *n*-propanol (△).

polyimide thin films are inversely proportional to alcohol molar volume. We believe that the diffusion rate of *n*-propanol in our films should also be smaller than ethanol. Thus, if *n*-propanol sorbs into all of the film surface area or free volume accessible to ethanol, the equilibration time for *n*-propanol should be greater than the time observed for ethanol. Since *n*-propanol equili-

brates faster, this suggests that the larger *n*-propanol molecules (kinetic diameter  $4.7 \text{ \AA}^{14}$ ) have less access to the film than do the smaller ethanol molecules (kinetic diameter  $4.3 \text{ \AA}^{14}$ ).

### Conclusions

Sol-gel processing techniques have been used to prepare zirconium acetate thin films that completely cover quartz substrates. Sorption studies indicate that the film interacts with alcohols through hydrogen bonding and essentially rejects alkanes. The combination of selective chemical interactions and surface area restrictions demonstrated by zirconium acetate films suggests that transition-metal carboxylate polymers are promising host materials for chemical sensor development. It should also be noted that these films are optically transparent and thus well suited to the fabrication of composite materials that combine the selectivity of an optical recognition center with the sorption selectivity of the porous glass matrix.

**Acknowledgment.** Financial support from the Center for Fundamental Materials Research at Michigan State University is gratefully acknowledged.

CM940469R